ESTRUCTURAS SECUNDARIAS DEL ADN: G-tetrads y G-quadruplexes

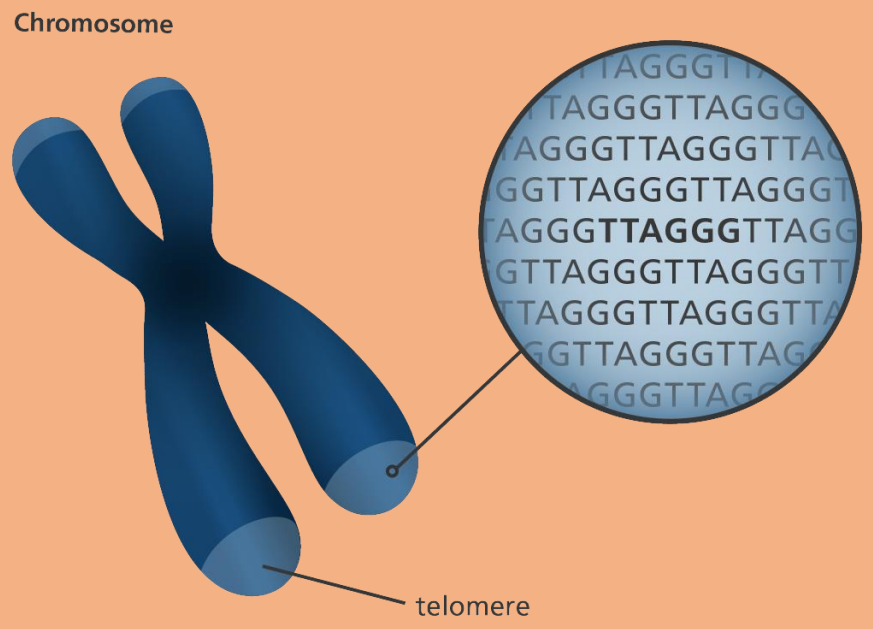

GFAyM-IMIT

Estructura del ADN

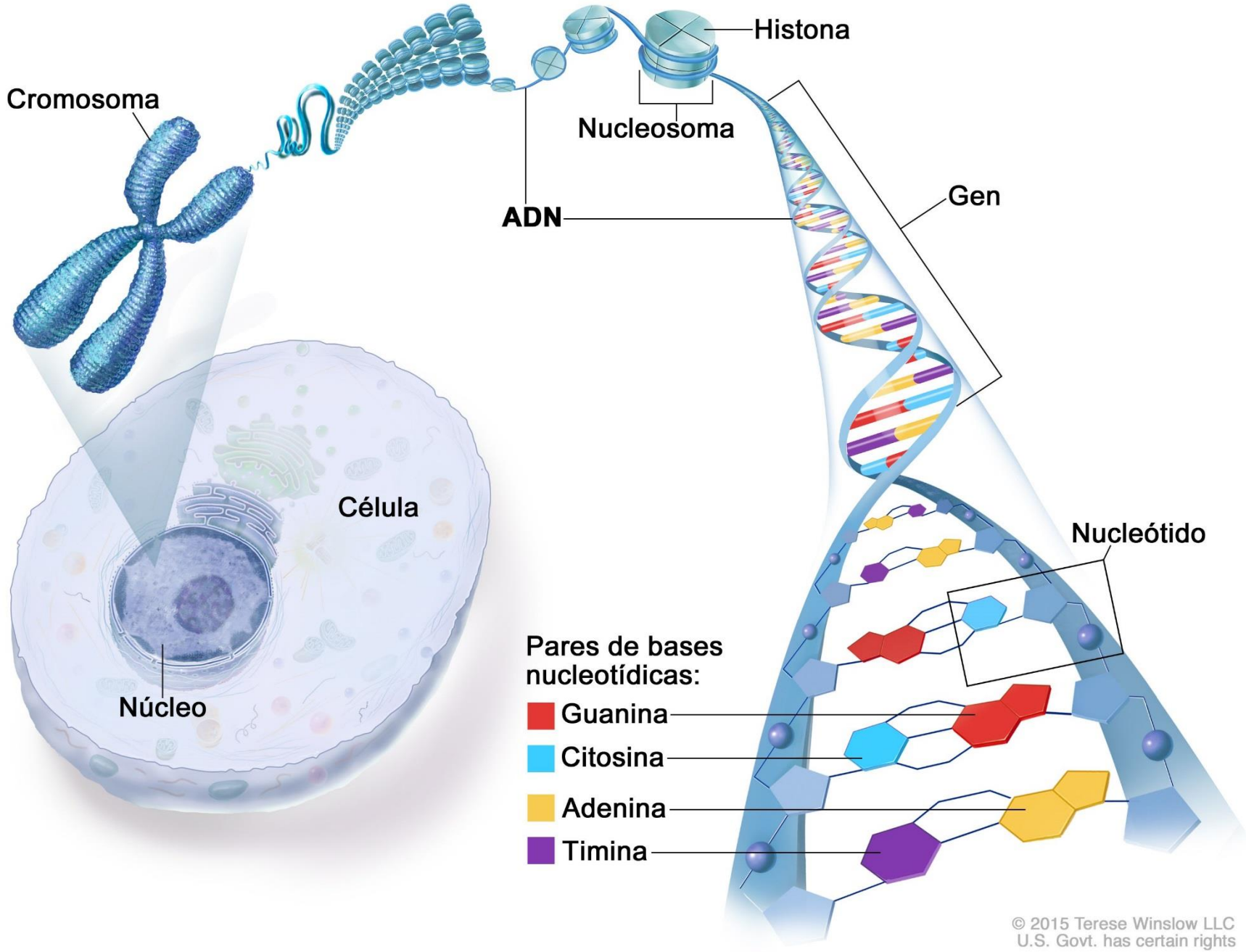

Duplex

G-Quadruplex

i-Motif

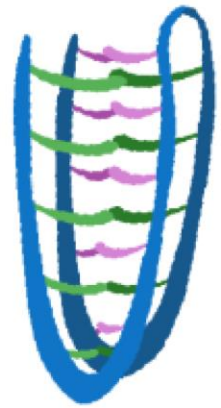

Triplex

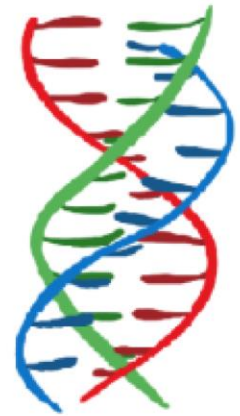

G-Triplex

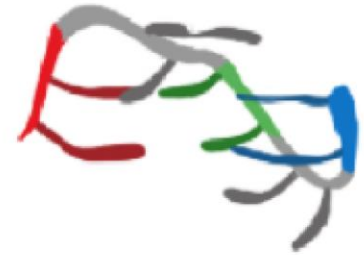

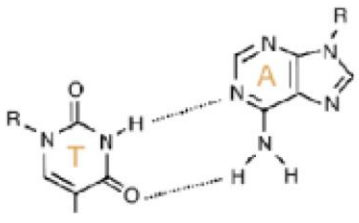

T-A base pair

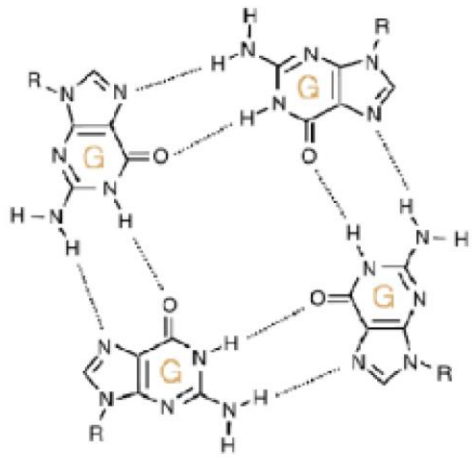

G-tetrad

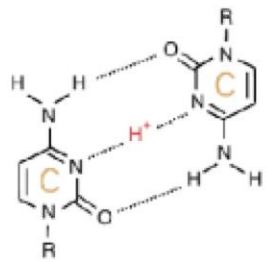

C-C+ base pair

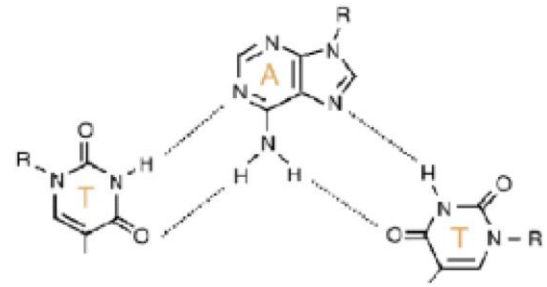

T-A:T triad

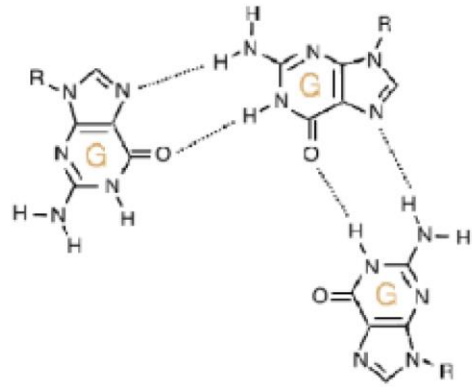

G-triad

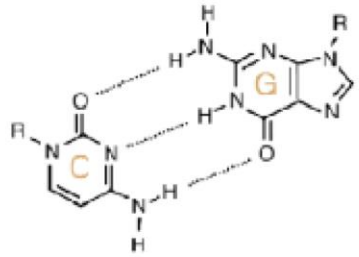

C-G base pair

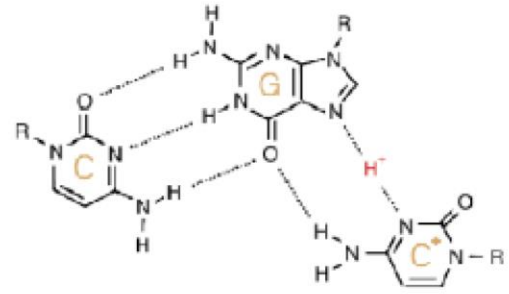

C-G:C⁺ triad

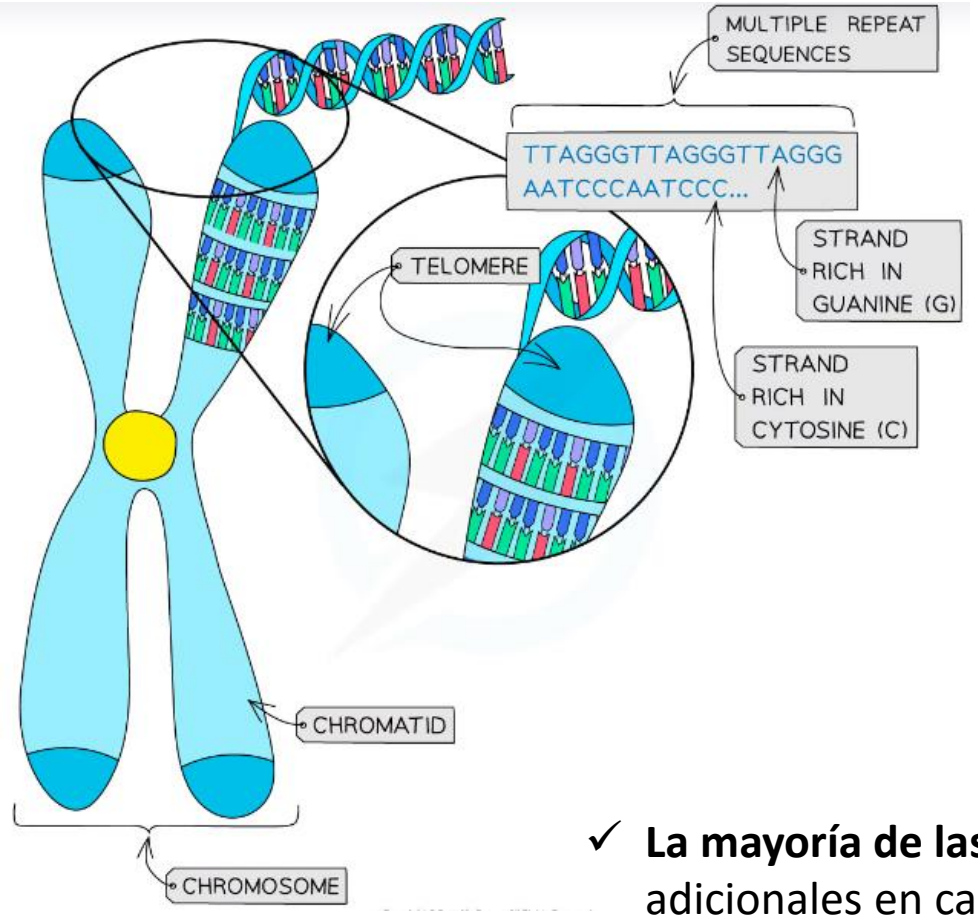

- ✓ Los extremos de las cromátidas en los cromosomas están "sellados" con estructuras protectoras llamadas **TELÓMEROS**.
- ✓ Están hechos de **ADN no codificante** que se compone de secuencias de bases cortas que se repiten muchas veces. Una **cadena es rica en G** y la otra cadena es rica en C.
- ✓ Función principal : **garantizar que los extremos del ADN se incluyan en la replicación del ADN durante la mitosis** (la enzima copiadora responsable de la replicación del ADN no puede llegar hasta el final de la molécula de ADN y se detiene un poco antes del fin).
- ✓ **Esto asegura que no se pierdan genes durante la división celular** (la pérdida de genes vitales puede incluso provocar la muerte celular) y permite la replicación continua de una célula.

- ✓ **La mayoría de las células tienen una enzima llamada telomerasa** que agrega bases adicionales en cada extremo (los telómeros). Algunas células (células especializadas) no disponen de telomerasa para ‘rellenar’ sus telómeros y por tanto tras un cierto número de divisiones celulares la célula muere, esto se ha relacionado con el proceso de envejecimiento.

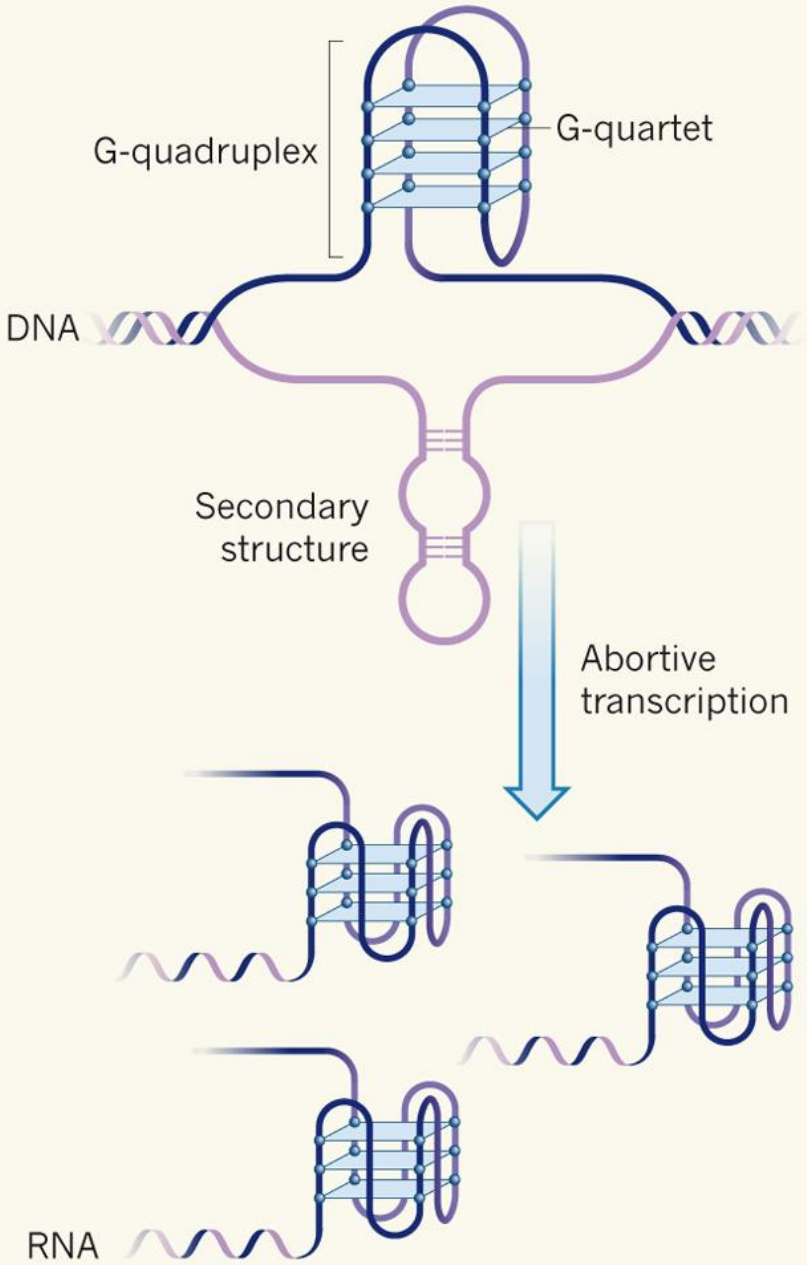
G-quadruplex
G-quartet
DNA
Secondary structure
Abortive transcription
RNA

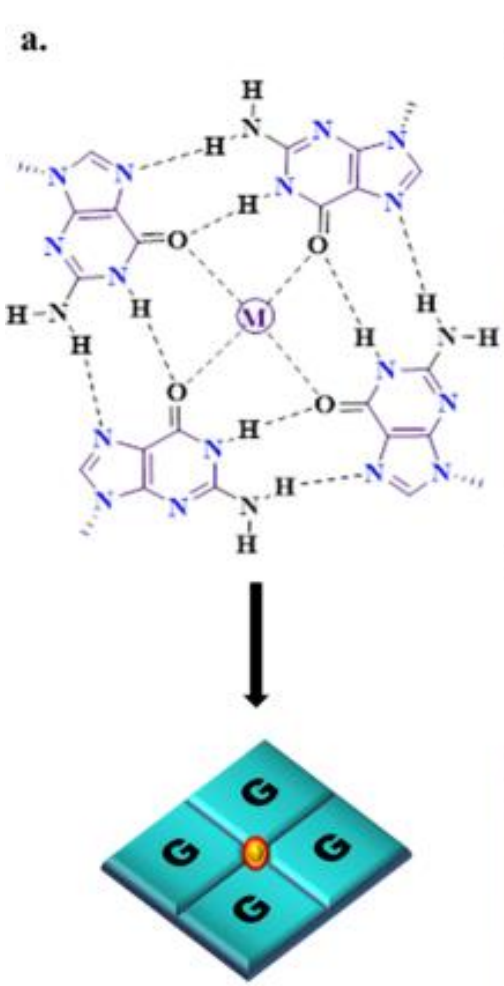
a.
M

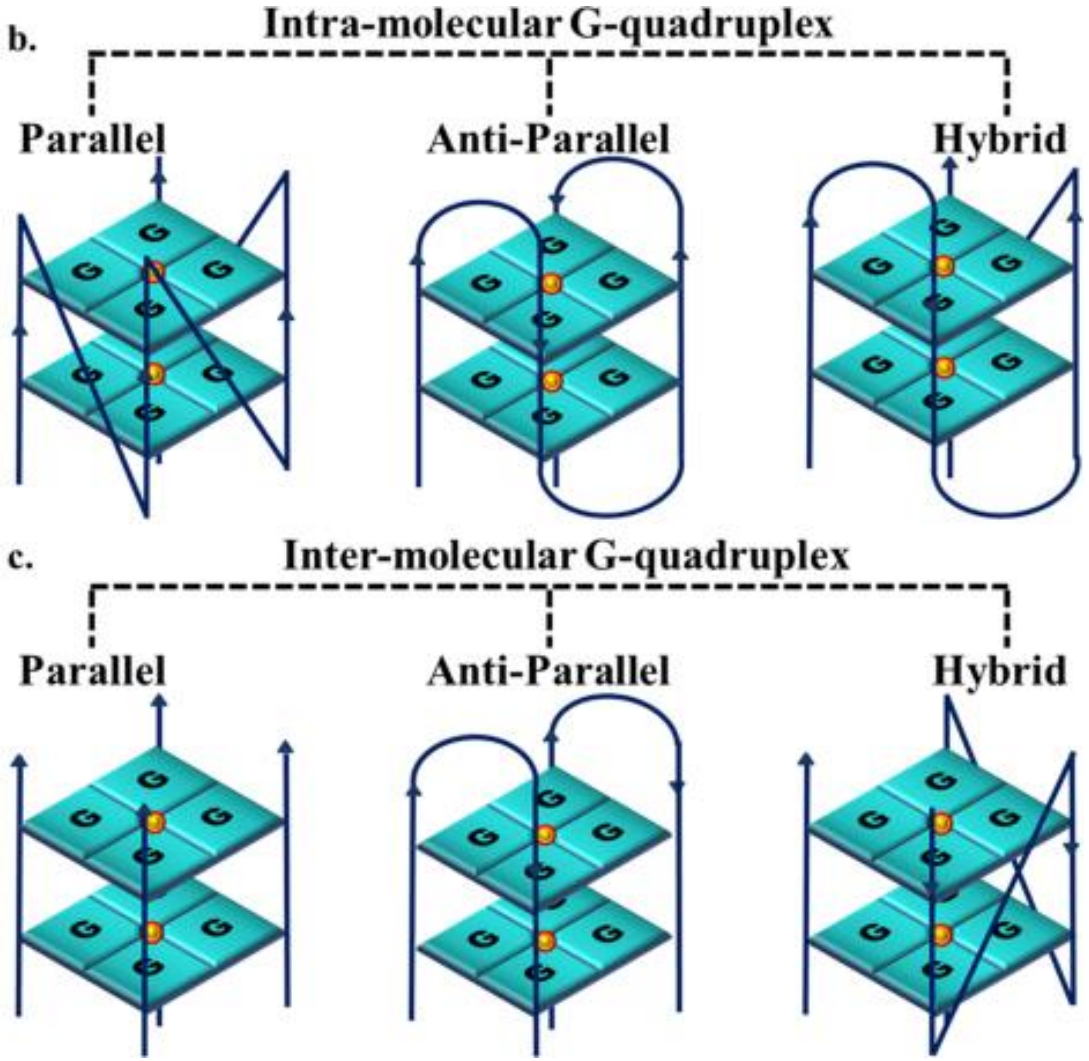
b.
Intra-molecular G-quadruplex
Parallel
Anti-Parallel
Hybrid
c.
Inter-molecular G-quadruplex
Parallel
Anti-Parallel
Hybrid

G-tetrad
Las bases de guanina forman tetrámeros planos estabilizados por una red de enlaces de hidrógeno de Hoogsteen

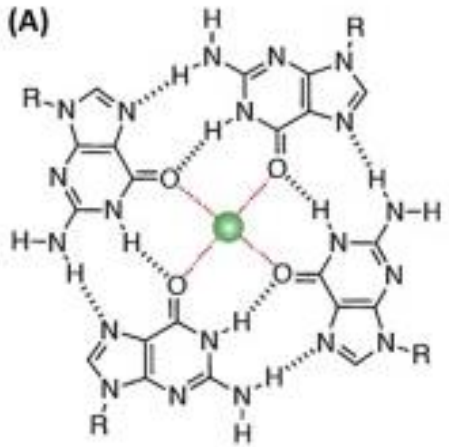

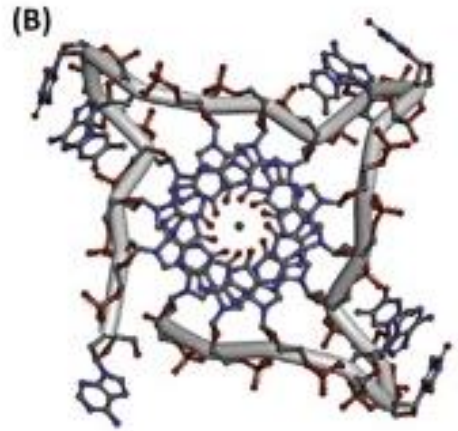

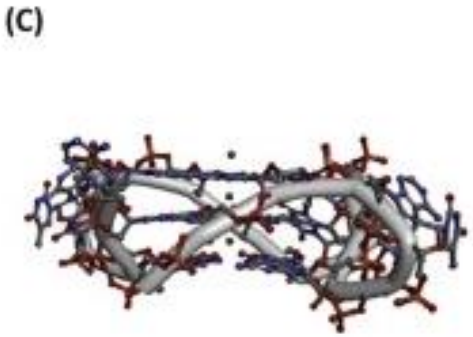

G-quadruplex
2, 3 o 4 láminas tetraméricas apiladas conducen a una estructura rígida que deja un canal central cargado negativamente, lo suficientemente grande como para albergar cationes estabilizadores (generalmente Na+ o K+).

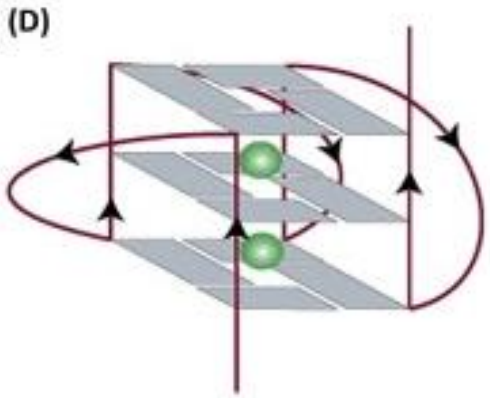

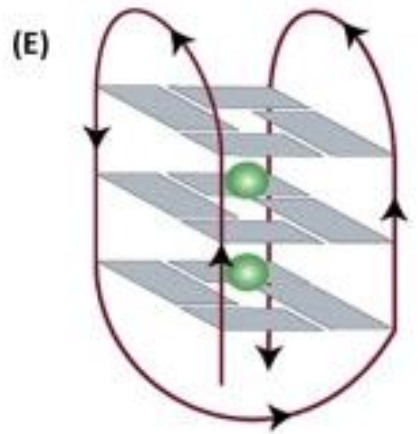

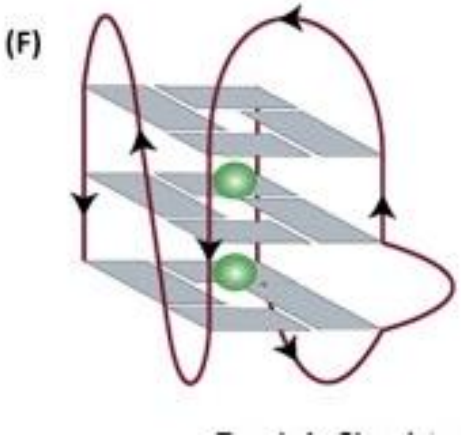

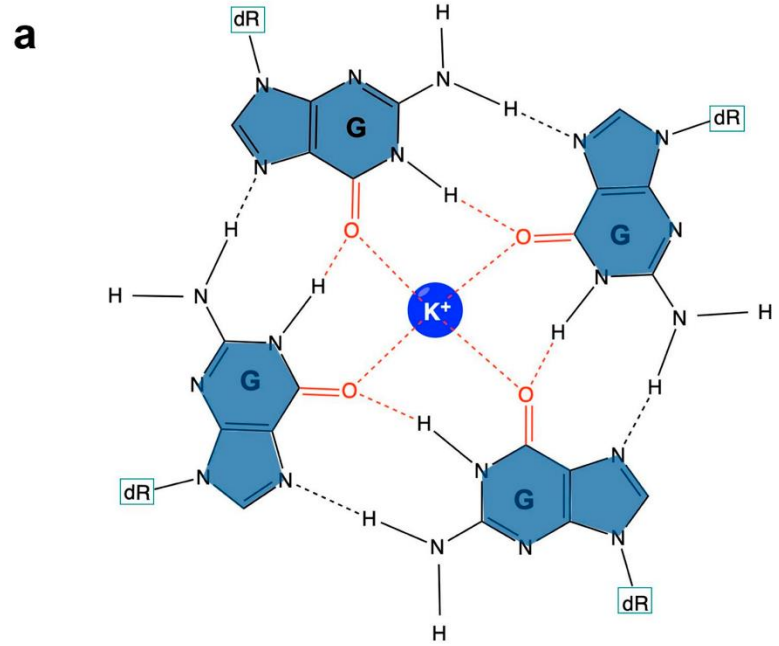

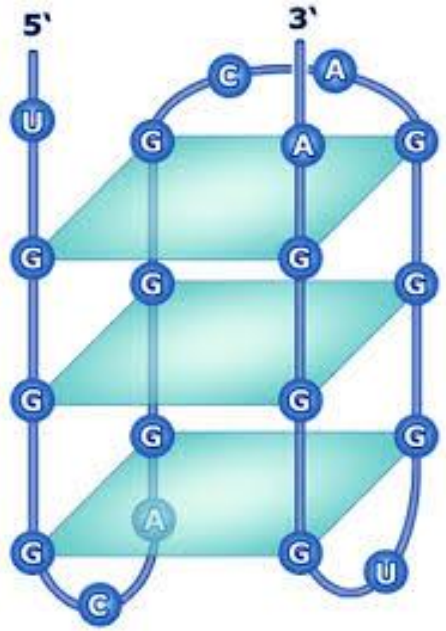

Existen regiones no codificantes etiquetadas inicialmente como ADN basura, pero que recientemente se ha descubierto que desempeñan un papel importante (funciones de regulación y estructurales).

Ventaja: El acortamiento de los telómeros está regulado por la interacción de la hebra con la telomerasa.
Desventaja: suele sobreexpresarse en una serie de tipos de cáncer invasivo.

Las **interacciones no covalentes** que implican anillos aromáticos, tales como enlaces de hidrógeno, EH, catión- π o stacking π-π, son cruciales para la estabilización de estas estructuras biomoleculares.

Uno de los principales objetivos del estudio de tales interacciones tiene que ver con la identificación de potenciales **drogas anticancerígenas o utilizables en el tratamiento de algunas enfermedades específicas.**

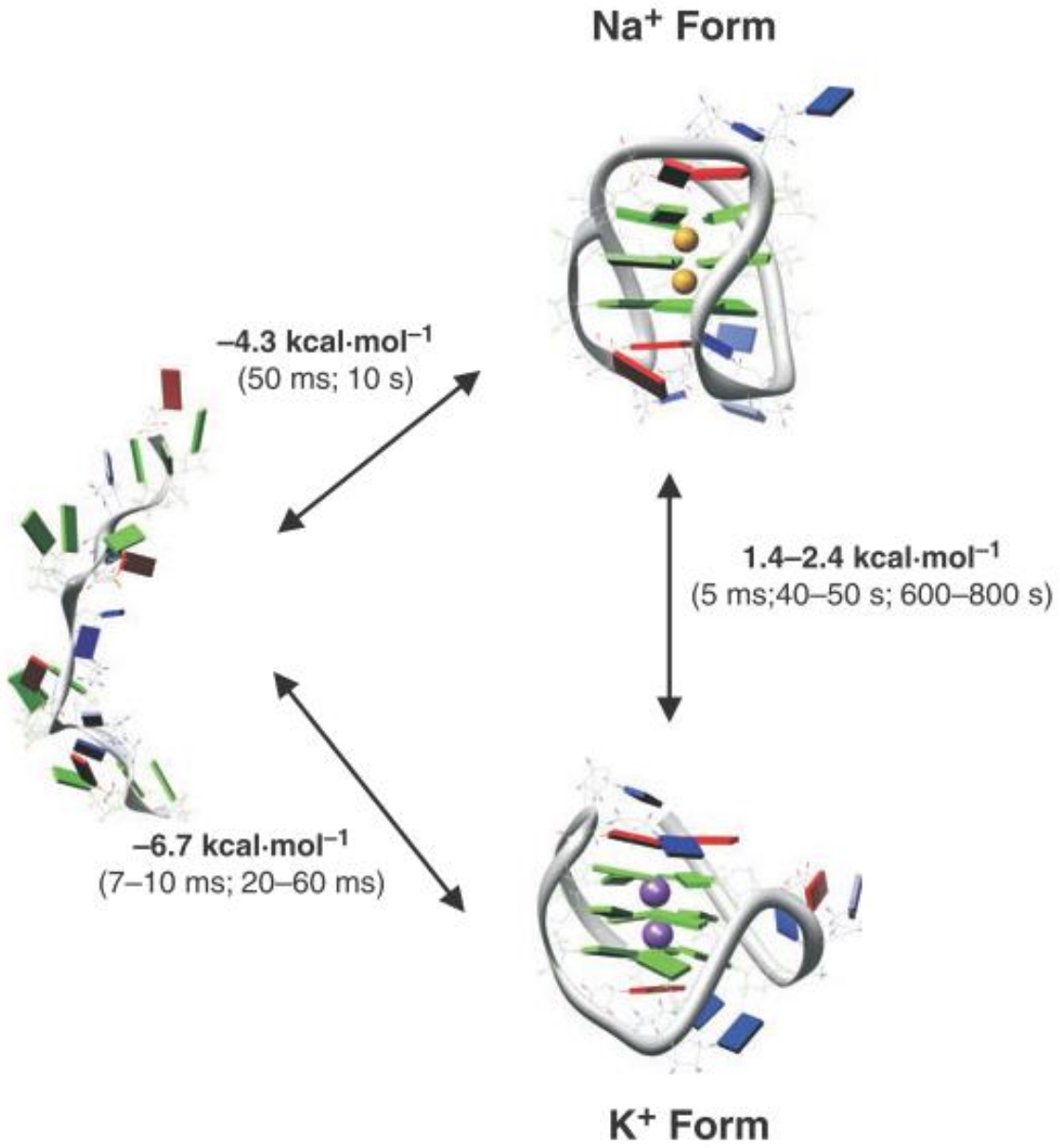

- ✓ El plegamiento y despliegue de las G-quadruplex no son simples procesos de dos estados, sino que proceden a lo largo de un camino con múltiples estados intermedios.
- ✓ Una vez formadas, las G-quadruplex pueden interconvertirse entre formas.
- ✓ Pequeñas barreras de energía separan las conformaciones de canasta e híbrida.
- ✓ De manera similar, el despliegue de las G-quadruplex requiere solo un modesto gasto de energía. Ese hecho puede ser de importancia biológica (ej: unión a proteínas para facilitar la replicación).

(a)

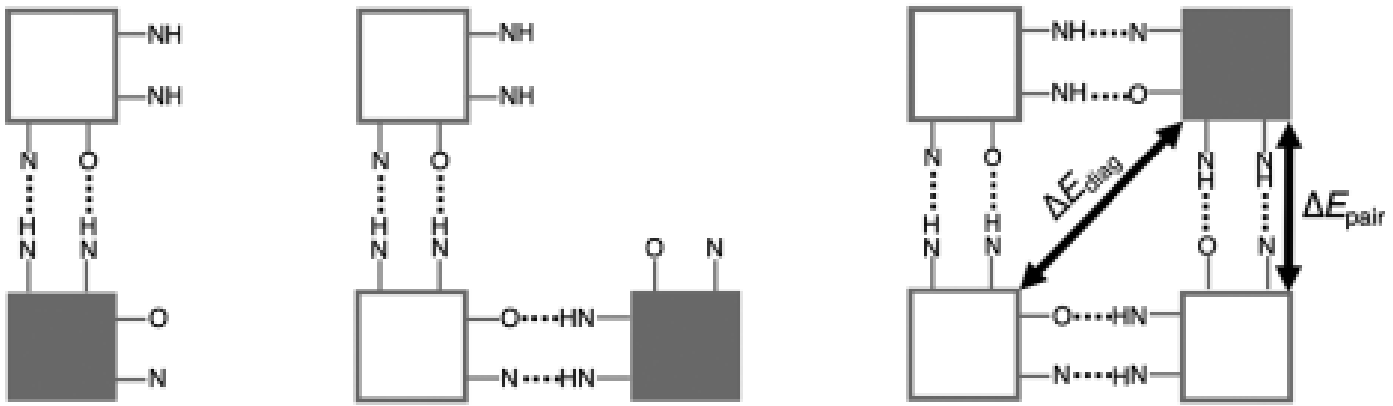

The cooperativity of the hydrogen bonds in G_4 was computed by comparing the interaction energy (ΔE_{int}) of the stepwise formation of the quartet from four guanine bases (in the geometry of G_4) with the sum of the individual pairwise interactions (ΔE_{sum}) for all possible pairs of bases in the G-quartet (see Equation 7).

$$\Delta E_{sum} = 4 \cdot \Delta E_{pair} + 2 \cdot \Delta E_{diag} \qquad (7)$$

TABLE 1

Energy Decomposition (in kcal mol^{-1}) of the Cooperative Stepwise Assembling of the G-Quartet (G_4)[a, b]

	G_2	G_3	G_4	G_2^{diag}	ΔE_{sum}	ΔE_{syn}[c]
ΔE_{oi}^{σ}	−14.7	−16.4	−36.1	−0.1	−59.1	−8.2
ΔE_{oi}^{π}	−1.8	−2.4	−6.2	−0.1	−7.3	−3.1
ΔE_{oi}	−16.5	−18.8	−42.3	−0.2	−66.4	−11.3
ΔE_{Pauli}	30.9	31.4	61.3	0.1	123.8	−0.2
ΔV_{elstat}	−26.4	−30.9	−60.9	−1.6	−108.8	−9.4
ΔE_{disp}	−4.5	−4.7	−9.1	−0.2	−18.3	0.0
$\Delta E_{int}(G_n)$	−16.5	−23.0	−51.1	−1.9	−69.7	−20.9

[a] Computed at ZORA-BLYP-D3(BJ)/TZ2P for frozen (fragments of) C_{4h}-symmetric G_4.

[b] Data taken from Ref. [63].

[c] Overall synergy in each energy term is defined as: $\Delta E(G_2)+\Delta E(G_3)+\Delta E(G_4)-4\,\Delta E(G_2)-2\,\Delta E(G_2^{diag})$.

ABBREVIATIONS AND DEFINITIONS

$\Delta E_{assemble}$	energy of assembly of the empty G-quadruplex scaffold
ΔE_{bond}	cation bond energy
ΔE_{disp}	dispersion energy
ΔE_{form}	energy of formation
ΔE_{int}	interaction energy
ΔE_{oi}	orbital interaction energy
ΔE_{Pauli}	Pauli repulsion energy
ΔE_{strain}	strain energy
ΔG_{form}	Gibbs free energy of formation
ΔQ	change in VDD atomic charge
ΔV_{elstat}	electrostatic interaction
ADF	Amsterdam Density Functional (program)
aq	aqueous solution
ASA	activation strain analysis
ASM	activation strain model
BJ	Becke–Johnson damping
BLYP	Becke exchange/Lee-Yang-Parr correlation functional
COSMO	conductor-like screening model
D3	Grimme's D3 dispersion correction
DFT	density functional theory

The formation of G-quadruplexes occurs when guanine-rich DNA or RNA single strands self-assemble in the presence of alkali metal cations. In the simplest example, one can form a double-layered GQ from four guanosine dimers (GG) and a metal cation M^+ (Figure 4). In quantum chemical analyses, the energy of formation (ΔE_{form}) associated with the formation of this double-layered G-quadruplex would be defined by Equation 9.

$$\Delta E_{\text{form}} = E\left(\text{GQ} - \text{M}^+\right)_{\text{aq}} - 4 \cdot E\left(\text{GG}\right)_{\text{aq}} - E\left(\text{M}^+\right) = \Delta E_{\text{assemble}} + \Delta E_{\text{bond}} \qquad (9)$$

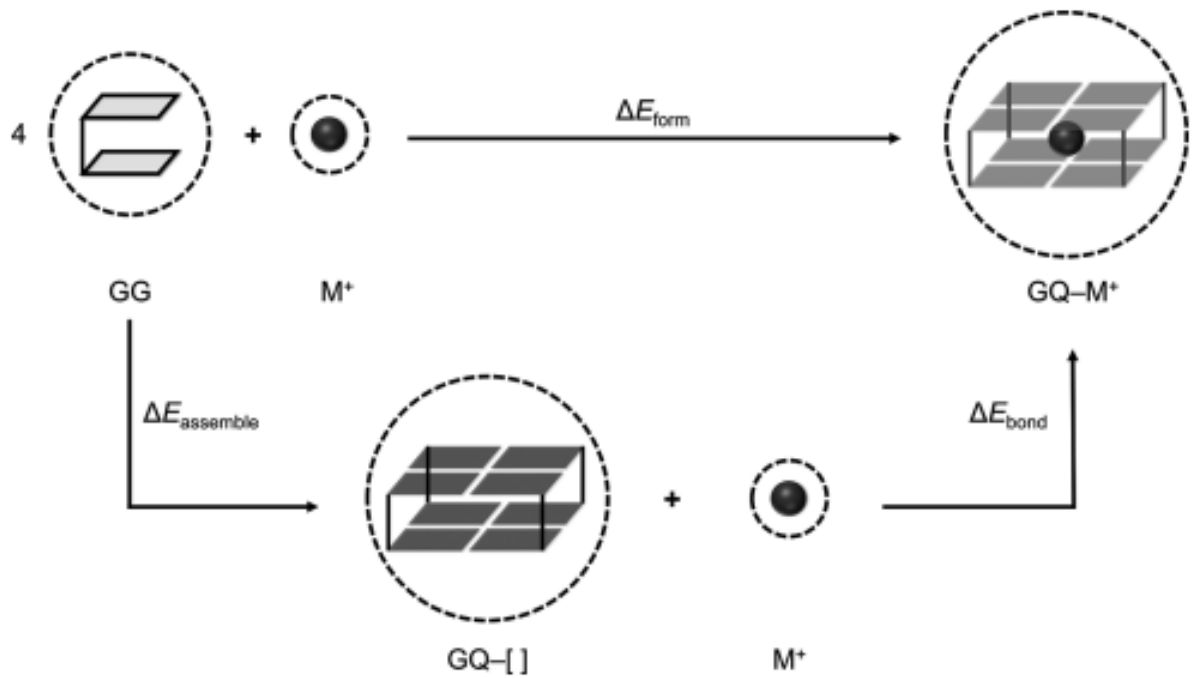

FIGURE 4 Partitioning of the energy of formation ΔE_{form} of a double-layer G-quadruplex. The dashed circles surrounding the structures indicate that the calculation is performed with COSMO to simulate solvation in water.

TABLE 2

Energy of Formation ΔE_{form} (in kcal mol^{-1}) of Double-Layer RNA and DNA G-Quadruplexes with and without Alkali Metal Cations (M^+)[a, b]

	$_{RNA}$GQ–M^+	$_{DNA}$GQ–M^+
M^+	ΔE_{form}	ΔE_{form}
No metal	−69.1[c]	−62.2[c]
Li^+	−106.2	−100.2
Na^+	−120.4	−114.5
K^+	−120.8	−115.4
Rb^+	−115.4	−111.1
Cs^+	−107.7	−103.1

[a] Computed at ZORA-BLYP-D3(BJ)/TZ2P.

[b] Data taken from Ref. [93].

[c] The energy of formation of the empty G-quadruplex (GQ–[ ]) corresponds to $\Delta E_{assemble}$.

[88, 94]. This phenomenon was hypothesized to be the result of the better stacking of the piled G-quartets in GQ-RNA [95] and the presence of additional intermolecular hydrogen-bond networks between the extra 2′-hydroxyl (OH) groups on the RNA ribose rings and the phosphate oxygen atoms of the sugar-phosphate backbone [96].

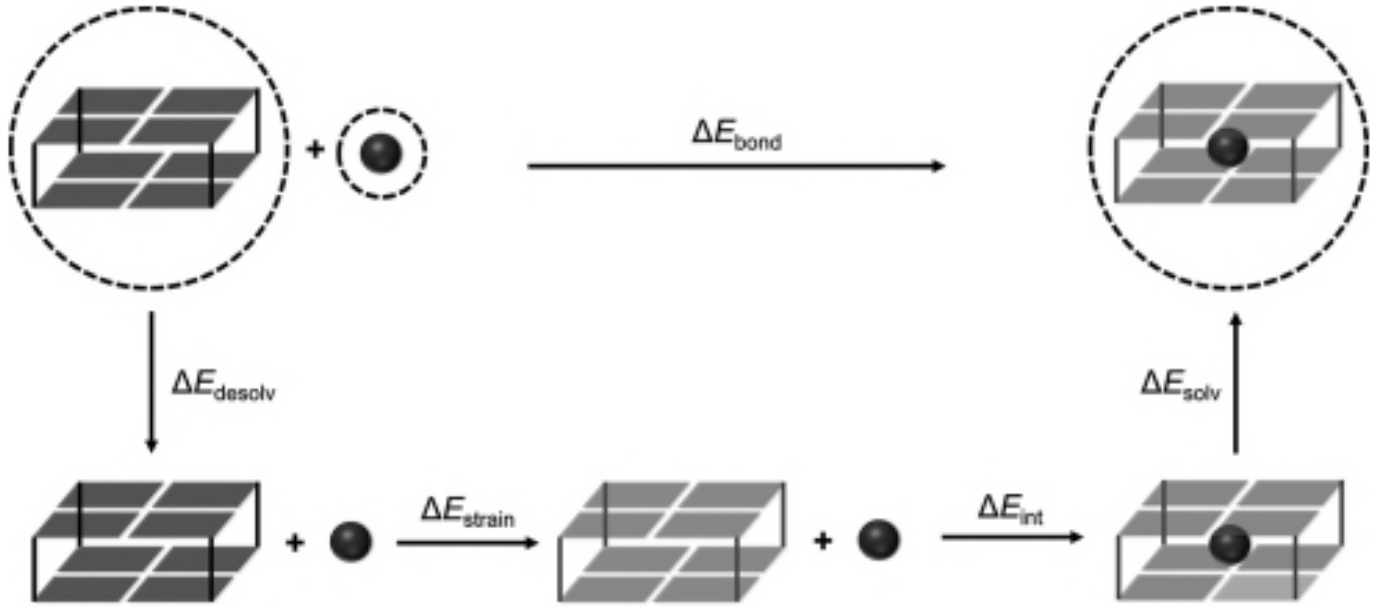

FIGURE 7 Partitioning of ΔE_{bond} of a metal cation (black sphere) binding to the central cavity of a double-layer G-quadruplex. The dashed circles surrounding the structures indicate that the calculation is performed with COSMO to simulate solvation in water.

These quantum chemical computations reproduced the experimental order of affinity with ΔE_{bond} becoming more stabilizing in the order $Li^+ < Rb^+ < Na^+ < K^+$ and obtained accurate G-quadruplex geometries in line with experimental geometrical parameters (e.g., hydrogen-bond and O6–M^+ distances). To understand the different components that determine the trend in the cation affinity, the bond energy was further decomposed into various energy terms as formulated by Equation 11 (see Figure 7 for a graphical representation of the energy terms).

$$\Delta E_{bond} = \Delta E_{desolv} + \Delta E_{strain} + \Delta E_{int} + \Delta E_{solv} \tag{11}$$

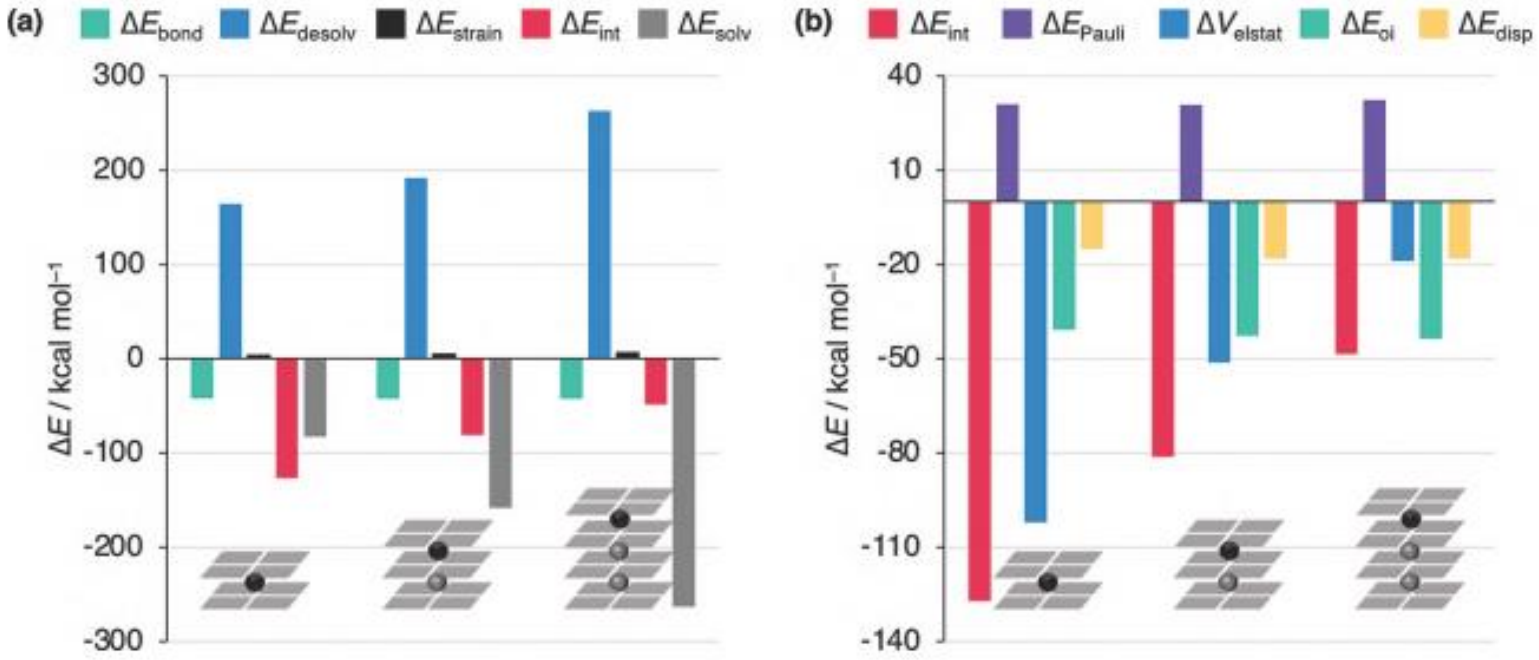

FIGURE 9 Partitioning of the (a) bond energy ΔE_{bond} and (b) interaction energy ΔE_{int} (in kcal mol^{-1}) for successive binding events of incoming K^+ cations (black spheres) in multi-layer G-quadruplexes. Gray spheres depict precoordinated K^+ cations. (Data taken from Ref. [33].)

The diminishing electrostatic attraction of the K^+ cations toward the GQ cavity is the result of the Coulombic repulsion between the incoming cation and the precoordinated cation(s) in the G-quadruplex. That the decrease in ΔV_{elstat} scales with the number of precoordinated cations implies that the electrostatic repulsion operates not only locally, that is, between directly neighboring cations, but also over longer distances, that is, for non-neighboring cations.

Y	Energy	B+B	B_2+B	B_3+B	B+B_{diag}	ΔE_{syn}[a]
G natural	ΔE_{oi}^{σ}	−14.7	−16.1	−36.2	−0.1	−8.0
	ΔE_{oi}^{π}	−1.7	−2.2	−6.0	0.0	−3.1
	ΔE_{oi}	−16.4	−18.4	−42.2	−0.2	−11.0
	ΔE_{Pauli}	30.6	29.9	60.7	0.1	−1.4
	ΔV_{elstat}	−25.9	−29.3	−59.8	−1.2	−9.0
	ΔE_{disp}	−4.6	−4.7	−9.3	−0.2	0.2
	ΔE_{int}[b]	−16.3	−22.5	−50.6	−1.4	−21.4
F	ΔE_{oi}^{σ}	−13.3	−14.8	−32.4	−0.1	−7.1
	ΔE_{oi}^{π}	−1.8	−2.4	−6.0	0.0	−3.0
	ΔE_{oi}	−15.1	−17.1	−38.4	−0.1	−10.0
	ΔE_{Pauli}	28.0	28.4	55.7	0.1	−0.1
	ΔV_{elstat}	−23.8	−27.8	−55.0	−1.3	−8.8
	ΔE_{disp}	−4.6	−4.8	−9.4	−0.2	0.0
	ΔE_{int}[b]	−15.5	−21.2	−47.1	−1.5	−18.8
Cl	ΔE_{oi}^{σ}	−14.0	−15.3	−34.0	−0.1	−7.1
	ΔE_{oi}^{π}	−1.9	−2.4	−6.2	0.0	−2.9
	ΔE_{oi}	−15.9	−17.7	−40.2	−0.2	−9.8
	ΔE_{Pauli}	29.4	28.9	58.5	0.1	−1.0
	ΔV_{elstat}	−24.5	−27.8	−56.4	−1.3	−8.1
	ΔE_{disp}	−5.2	−5.4	−10.7	−0.2	−0.1
	ΔE_{int}[b]	−16.3	−22.1	−48.7	−1.5	−18.9
Br	ΔE_{oi}	−16.2	−18.0	−40.9	−0.2	−9.9
	ΔE_{Pauli}	29.6	29.0	58.7	0.1	−1.3
	ΔV_{elstat}	−24.5	−27.6	−56.2	−1.2	−7.9
	ΔE_{disp}	−5.5	−5.7	−11.2	−0.2	0.0
	ΔE_{int}[b]	−16.6	−22.4	−49.5	−1.5	−19.1
I	ΔE_{oi}	−16.6	−18.5	−41.7	−0.2	−10.0
	ΔE_{Pauli}	30.4	29.9	60.5	0.1	−1.0
	ΔV_{elstat}	−24.8	−27.9	−56.7	−1.2	−7.8
	ΔE_{disp}	−5.9	−6.1	−12.0	−0.2	0.0
	ΔE_{int}[b]	−16.9	−22.6	−50.1	−1.4	−19.2